

Triggering with the ALICE TRD

Jochen Klein^a, for the ALICE collaboration

^a*Physikalisches Institut, University of Heidelberg, Philosophenweg 12, 69120 Heidelberg, Germany*

Abstract

We discuss how a level-1 trigger, about 8 μ s after a hadron-hadron collision, can be derived from the Transition Radiation Detector (TRD) in A Large Ion Collider Experiment (ALICE) at the LHC. Chamber-wise track segments from fast on-detector reconstruction are read out with position, angle and electron likelihood. In the Global Tracking Unit up to 6 tracklets from a particle traversing the detector layers are matched and used for the reconstruction of transverse momentum and electron identification. Such tracks form the basis for versatile and flexible trigger conditions, e.g. single high- p_{\perp} hadron, single high- p_{\perp} electron, di-electron (J/Ψ , Υ) and at least n close high- p_{\perp} tracks (jet).

The need for low-latency on-line reconstruction poses challenges on the detector operation. The calibration for gain (pad-by-pad) and drift velocity must be applied already in the front-end electronics. Due to changes in pressure and gas composition an on-line monitoring and feedback loop for these parameters is required. First experiences on the performance were gathered from triggering in cosmic and pp runs.

Keywords: ALICE, TRD, trigger

1. Introduction

The design of the ALICE TRD was driven by the requirement for very good pion rejection in the high multiplicity environment of Pb–Pb collisions and by the goal to use the information for a fast trigger contribution. Many interesting probes, such as J/Ψ , Υ , open heavy-flavour, have (semi-)electronic decay channels. For their analysis good electron identification is of crucial importance. As these probes are rare, triggering is essential to record a sufficient sample of events. Covering $[-0.9, 0.9] \times 2\pi$ in η - φ , the scope of the trigger extends beyond electron channels, e.g. to jets.

The detector is segmented into 18 super-modules in azimuth, each comprising 5 stacks of 6 layers of tracking chambers. Each chamber consists of a radiator, a drift volume and a multi-wire proportional chamber with pad read-out [1]. In this design a short drift could be combined with the possibility of local chamber-wise tracking. For efficient absorption of the transition radiation photons Xe is used as counting gas, with a 15 % admixture of CO_2 as quencher. The front-end electronics is mounted directly on the chambers. The general setup and performance of the TRD and its physics applications were discussed in other contributions at this meeting [2, 3].

In section 2 the general concept of the TRD triggers is described providing an overview of the steps involved. The subsequent section explains the on-line reconstruction in more detail. Sections 4 and 5 describe the simulation

framework and the observed performance, respectively. In section 6 a TRD trigger on jets is discussed.

2. TRD-based triggering

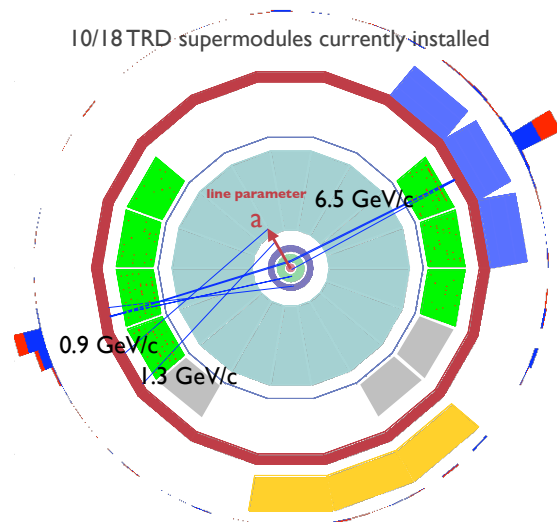


Figure 1: An event display showing two back-to-back jets of about 45 GeV. The blue lines show the global tracks reconstructed as straight line fits through the TRD tracklets. The line parameter a is used to extract the transverse momentum.

In ALICE three levels of hardware triggers are used. At the first stage level-0 contributions from fast detectors, such as scintillators and silicon pixel detectors, are evaluated by the Central Trigger Processor (CTP) to issue

Email address: jklein@physi.uni-heidelberg.de
(Jochen Klein)

| trigger | time | rate |
|---------|------------------------|------------------------|
| level-0 | $\sim 1.2 \mu\text{s}$ | $\sim 100 \text{ kHz}$ |
| level-1 | $\sim 7.7 \mu\text{s}$ | $\sim 2.5 \text{ kHz}$ |
| level-2 | $\sim 100 \mu\text{s}$ | $\sim 1.5 \text{ kHz}$ |

Table 1: Overview of the hardware trigger stages used in ALICE. The three hardware levels are followed by a computing cluster forming the High-Level Trigger [4].

a level-0 trigger. The set of triggered detectors depends on the combination of fired trigger inputs. $6.5 \mu\text{s}$ after a level-0 trigger the read out can be continued or aborted depending on the contributions to the level-1 trigger. So far, the ElectroMagnetic CALorimeter (EMCAL), the Zero-Degree Calorimeter (ZDC) and the TRD contribute at that level. After the drift time of the time projection chamber ($\sim 90 \mu\text{s}$) the read-out must be accepted or rejected by a level-2 decision. This mechanism is mainly intended for the rejection of events with too many pile-up interactions (past-future protection) but could also be used for more complex triggers. The trigger chain is completed by the High-Level Trigger (HLT) implemented in a computing cluster. It processes the data from all events which have been accepted at level-2. For an overview of possible rates at the different trigger stages see Table 1.

Data from the TRD become available only after the acquisition has been initiated by a level-0 trigger. Therefore, a high level-0 rate is needed to sample a large number of events with the TRD triggers. They are based on tracks which are reconstructed on-line from TRD data only. First, local track segments, so-called tracklets, are calculated in every chamber. Those are shipped via optical links to the Global Tracking Unit (GTU). To achieve low latencies all tracklets must be accepted without backpressure. The tracklet read-out is sorted such that the matching can be performed as the data arrive. For found tracks the transverse momentum is extracted from a straight line fit as the offset to the primary vertex.

By using the tracks as basis for the trigger decision a variety of signatures can be used. A trigger on a single high- p_{\perp} particle, on top of a level-0 condition based on TOF, has been used for cosmic data taking. In this way a very pure sample of tracks could be provided for the analysis of very high momentum cosmic muons [5]. Asking for several tracks above a p_{\perp} threshold in a small $\eta - \varphi$ area allows to trigger on jets. The selection of identified electrons above a p_{\perp} threshold allows to enhance events with semi-leptonic decays of heavy flavour mesons. The di-electron signature shall be used to select events with electronic decays of J/Ψ or Υ .

3. On-line reconstruction

3.1. Local tracking

When a charged particle traverses a TRD chamber (see Fig. 2) it deposits energy by ionization of the gas in the

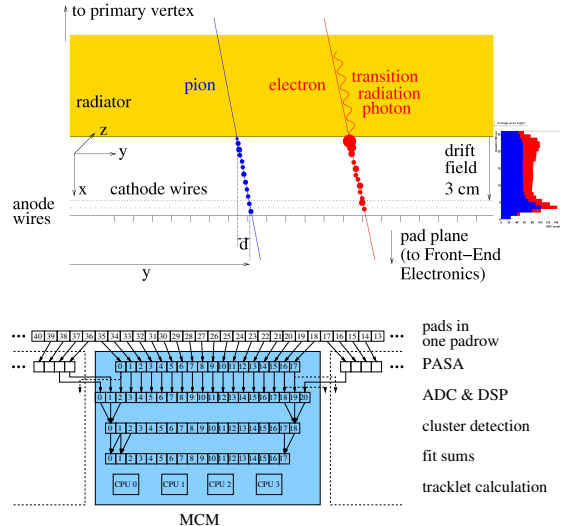


Figure 2: Top: Cross section of a TRD chamber. Depending on its Lorentz γ a charged particle traversing the radiator can emit transition radiation which is absorbed within the drift region. Together with the electrons from ionisation of the gas the signal is detected in a MWPC. The pads are read out by front-end electronics mounted on the back of the chamber. Bottom: The processing of the pad singals. The charge-sensitive PASA feeds the ADCs in the TRAP. The edge channels are shared among adjacent chips. A preprocessor prepares the data for the final tracklet fit by the CPUs.

active volume of the detector. Furthermore, highly relativistic particles with a Lorentz factor $\gamma \gtrsim 1000$ can emit transition radiation in the radiator material consisting of a fibre/foam sandwich [1]. Because of the high photoabsorption cross section in Xe such a photon with X-ray energy is absorbed most likely close to the entrance to the drift volume. Except for very energetic particles, e.g. cosmic muons, the characteristic additional energy deposit at the end of the drift time can be exploited for the identification of electrons.

The electrons from ionization of the gas drift towards an amplification region which is separated from the drift volume by a cathode wire grid. Induced signals are read out from a cathode pad-plane. Its granularity is fine in the transverse direction ($\sim 1 \text{ cm}$), while it is coarse along the beam direction ($\sim 10 \text{ cm}$). Therefore, the y -position (bending direction) can be determined accurately for individual clusters. To recover the z -position during off-line tracking the pads are tilted by $\pm 2^\circ$ degrees with the sign alternating from one layer to the next.

The signal from the pads is fed to the front-end electronics mounted on the backside of the pad plane. Groups of 18 channels are connected to a Multi-Chip Module (MCM) with two ASICs. The output of the charge-sensitive PreAmplifier and Shaping Amplifier (PASA) is fed to the TRacklet Processor (TRAP). To avoid inefficiencies for the on-line tracking the edge channels are shared between adjacent TRAPs as shown in Fig. 2. The signals are digitized by ADCs with a sampling frequency of 10 MHz. With a drift velocity around $1.5 \frac{\text{cm}}{\mu\text{s}}$ the full signal

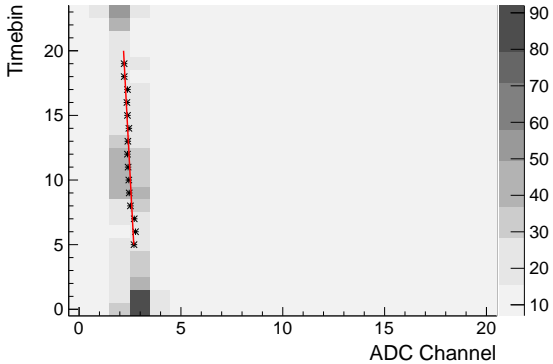


Figure 3: Processing of the ADC data within one MCM. The digitized values are searched time bin wise for clusters, i.e. charge in three adjacent channels. The calculation of the hit position (asterisks) takes into account the pad response function. If a sufficient number of clusters is found in two adjacent channels a tracklet fit is calculated as straight line.

extends over 20 time bins. Typically, 24 time bins are read out to cover both the rising and falling edge of the signal, which are needed e.g. for the drift velocity calibration.

The data pass through a chain of digital filters. A pedestal filter subtracts the channel-specific baseline as obtained over a long sampling period. A common baseline is added again to allow for the detection of undershoots created in later filter stages. Gain variations can be corrected for each of the 1.3 million channels by applying a correction:

$$O_n(t) = \gamma_n \cdot I_n(t) + \alpha_n \quad (1)$$

where n denotes the channel number. Because the multiplicative correction γ_n also affects the common baseline an additive correction α_n is needed to readjust the baseline. The so-called gain tables with the correction values for all channels are obtained from calibration runs with meta-stable Krypton added to the gas system [6] and are loaded during the initialization of the front-end electronics. In a tail cancellation filter the ion tails are suppressed by subtraction of two exponentials:

$$S(t) = 1_{(t \geq 0)} \cdot (\alpha_L \lambda_L^t + (1 - \alpha_L) \lambda_S \lambda_S^t) . \quad (2)$$

Both the decay rate and the relative contribution are configurable as λ_L , λ_S , and α_L [7].

The filtered data are searched timebin-wise for clusters (see cluster detection in Fig. 2). To find a cluster the charge on three adjacent pads must exceed a configurable threshold. In addition, the central pad must have the highest signal. For every found cluster a position is calculated as the centre of gravity of the charges to which a correction from a configurable look-up table is added. This look-up table is filled with values obtained from the known pad response functions. The data available at that stage is shown in Fig. 3.

Later, the clusters shall be used for linear fitting. Therefore, the needed sums of X , X^2 , Y , Y^2 and, XY are accumulated during the processing for all channels in parallel.

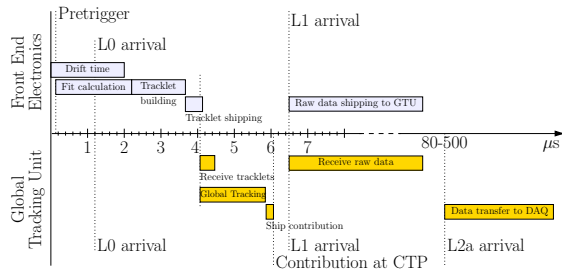


Figure 4: Timing requirements for the on-line reconstruction. The electronics is woken up by a pretrigger signal shortly after the interaction. Only for a level-0 accept the tracklet calculation proceeds. The raw data readout only starts after a level-1 trigger.

Each cluster is stored according to its central channel. X denotes the time bin and Y the position in units of pad widths.

To keep the noise level low the CPUs are only started after the drift time and, thus, after the sampling. For each pair of adjacent channels the numbers of hits is counted over all time bins in a configurable range. If a minimum number of hits is exceeded the tracklet calculation is performed. Up to four candidates can be processed by the CPUs. Position and slope are calculated from the accumulated fit sums.

Initially, the slope is calculated per timebin. To obtain the deflection d (see Fig. 2) it is multiplied by the drift velocity and the drift length of 3cm. In addition, it is corrected for the Lorentz drift and the pad tilt. A cut on the deflection is applied to reject tracklets from low p_{\perp} tracks. If the cut was passed the final information of a tracklet is packed into a 32-bit word and shipped over the optical read out tree to the Global Tracking Unit.

The temporal sequence of the various steps is shown in Fig. 4. After receipt of a pretrigger the full drift time can be sampled because of pipeline stages in the digital filtering. The fit sums are calculated during the drift time, but the CPUs only start after the end of the drift time. The tracklets are processed in the GTU while arriving. If a given signature was found the trigger contribution is shipped to the CTP. The raw data readout only starts after a level-1 trigger was received.

3.2. Global Tracking

The global tracking is implemented in an array of FPGAs [8]. Upon arrival at the Global Tracking Unit (GTU) the tracklets are grouped according to their z -position. The subsequent matching stage only considers combinations of tracklets that are consistent with a track pointing to the primary vertex in the longitudinal direction. The tracklets are projected to a reference plane. If tracklets from at least 4 layers fall into a close region they form a track. For sets of matched tracklets the p_{\perp} reconstruction is performed by calculating a straight line fit through the tracklet positions in the transverse direction. The line parameter a is translated into the transverse momentum. An overview of the procedure is given in Fig. 1.

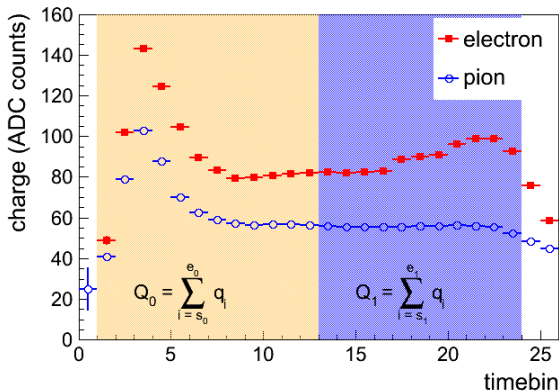


Figure 5: The on-line electron identification is based on the charge accumulated in two configurable time windows. The tracklet PID for Q_0, Q_1 is then looked up from a table loaded to the TRAP memory. It is also possible to use only one window and use the total charge for the PID.

3.3. Electron identification

Electron likelihoods are carried along through the tracking chain. For each tracklet the charge of found clusters is summed within two configurable time windows during local tracking as illustrated in Fig. 5. Then, a look-up table is used to translate these charges into an electron likelihood. For the global particle identification used for track selection in trigger conditions, the likelihoods from the tracklets are averaged in the Global Tracking Unit.

For the extraction of reference spectra from real data samples of topologically identified electrons and pions, e.g. from $\gamma \rightarrow e^+e^-$ or $K^0 \rightarrow \pi^+\pi^-$, are used. A one-dimensional look-up table using the total charge of a tracklet is used at the moment to reduce the required statistics for the reference data extraction.

In Monte-Carlo simulations the look-up table can be generated from the signals observed for particles of known species. Then, thresholds can be defined to achieve a given efficiency for identifying electrons as such. The performance can be evaluated by extracting the resulting pion rejection. Fig. 6 shows the performance for the one-dimensional method from a study using the tracklet simulation discussed in the next section [9].

4. Simulation

With the complex processing in multiple stages of the detector it was crucial for debugging and understanding to have an exact simulation of the hardware components. For both the local and the global tracking, models have been implemented in AliRoot [10, 11] which simulate the behaviour of the electronics by performing exactly the same operations. Not only can this simulation be used in pure Monte-Carlo events but also on recorded data. This is because the trigger is completely based on ADC data which are also read out for accepted events. In Fig. 7 the different types of data are shown. In addition to the ADC

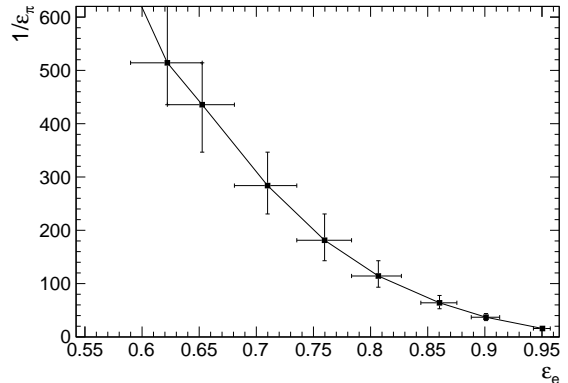


Figure 6: Pion rejection in Monte-Carlo simulation. The likelihood threshold to identify a particle as an electron is chosen such that a given electron efficiency ϵ_e is achieved. The resulting pion rejection $1/\epsilon_\pi$ can then be extracted (adapted from [9]).

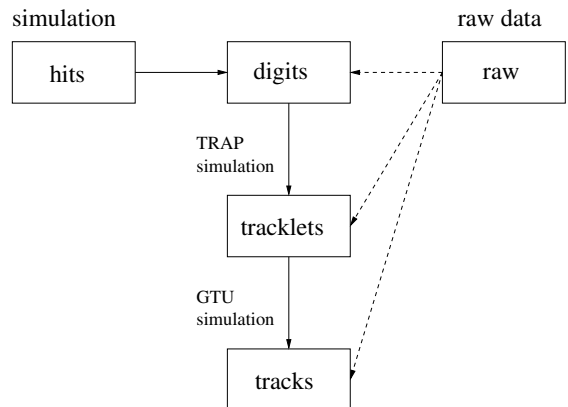


Figure 7: Trigger information in raw data and simulation. During reconstruction the ADC values, tracklets and tracks are extracted from raw data. The TRAP and GTU simulations allow to recalculate the tracklets and tracks from these data. In the pure Monte-Carlo case the ADC values (digits) are derived from detector hits.

values (digits) the raw data contain the tracklets and the tracks as calculated in the detector electronics and used for triggering. The simulation can be used to recalculate and compare them to the actual results.

Also the configuration of the TRAP with all registers and memory blocks is exactly modelled in AliRoot such that a configuration from the Detector Control System [12] can be used identically. This allows to perform simulations with the exact configuration as used in the actual data taking.

It has been very useful for debugging and understanding to have this simulation chain available, which agrees on the bit-level with the data read out from the actual detector. With identical configurations any deviation between simulation and real data points to a problem. On the other hand, the effect of parameter changes can be studied much quicker in the simulation.

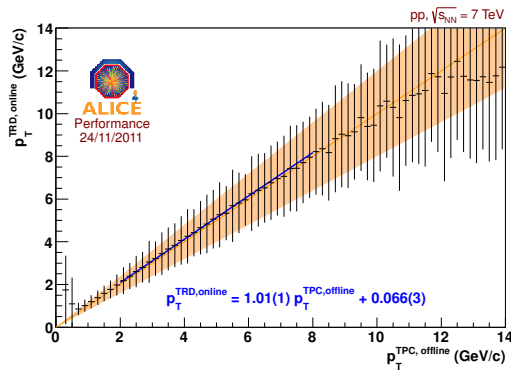


Figure 8: The correlation of the transverse momenta is shown for on-line tracks matched to a TPC track. The data point is the mean of the distribution and the error bars show the standard deviation.

5. Tracking performance

5.1. Monte-Carlo

Using the simulation of local and global tracking explained in the previous section it is possible to evaluate the performance based on events from pure Monte-Carlo generators. The tracklets can be assigned to known particle trajectories by labels such that position and deflection can be compared to Monte-Carlo truth. This has mainly been used to understand the influence of configuration changes, e.g. the impact on the electron identification.

5.2. Refit to data

The tracking results in the raw data do not only contain the final parametrization but also the references to the contributing tracklets. Hereby, it is possible to perform a helix fit through the contributing tracklets and calculate the residuals. Since no other data but TRD trigger information are needed this can be used as a quality measure for on-line monitoring.

5.3. Comparison to off-line tracking

When the full off-line information is available, tracks reconstructed in the time projection chamber can be used as reference. They are geometrically matched to the GTU tracks by the position of contributing tracklets. Then, the parameters obtained from the on-line reconstruction can be compared to the off-line reconstruction. This is shown for the transverse momentum in Fig. 8 based on recently recorded data. As expected the transverse momenta from on-line and off-line reconstruction are correlated. With 20 % the spread is still larger than the design goal. This is due to non-optimal settings in the front-end electronics, e.g. mis-alignment is not yet corrected for.

In a similar way the overall tracking efficiency is determined. The denominator is formed by tracks having at least four tracklets in one TRD stack. Tracks found in the GTU and matched to a findable one are considered for the

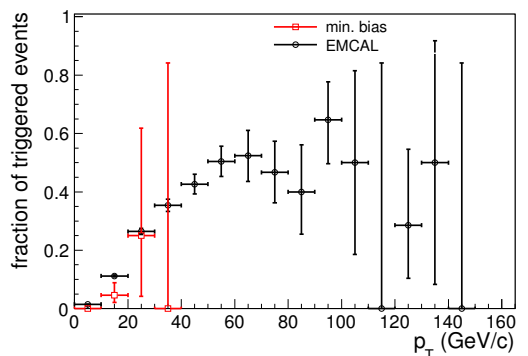
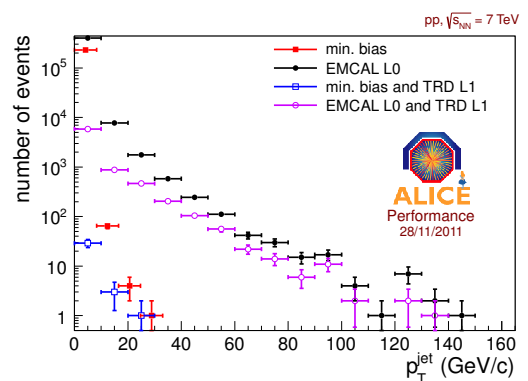


Figure 9: Top: The raw jet spectra are shown for a minimum bias and an EMCAL-triggered event sample. In both cases also the spectrum for which the trigger condition was fulfilled is plotted. Bottom: The efficiency of the jet trigger can be extracted from comparison of the triggered and untriggered spectra.

efficiency calculation. This is done to separate the trigger-specific efficiency from other effects such as the detector acceptance. For tracks above 3 GeV/c this efficiency is found to be above 90 %.

6. Jet trigger

The area covered by a TRD stack in the η - φ plane is comparable to the area of a typical jet cone. Therefore, a jet can be characterized by a number of tracks within such an area and a jet trigger can be realized by requiring a minimum number of tracks above a p_{\perp} threshold within any TRD stack. This works despite the fact that only charged tracks are amenable to the TRD reconstruction. From Monte-Carlo checks we expect the trigger to become fully efficient from jet energies around 100 GeV/c on, depending on the condition used.

Requiring 3 tracks above 3 GeV/c in any TRD stack was found to be a suitable condition to trigger on jets. Fig. 10 shows the rejection of minimum bias events for different combinations of the minimum number of tracks and the applied p_{\perp} threshold. The various conditions were evaluated on the tracks in raw data. The above threshold results in a good rejection of about 10^4 .

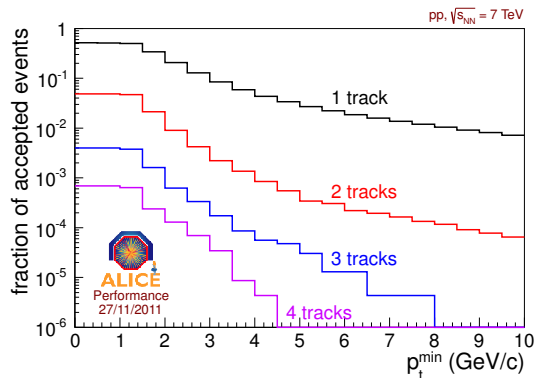


Figure 10: The rejection of minimum bias events is extracted for different thresholds in the jet trigger condition. The different lines correspond to different minimum numbers of tracks whereas the abscissa shows the required p_{\perp} .

To check that the jet trigger works as expected, a sample of pp collisions at $\sqrt{s} = 7$ TeV was used. The events were classified according to the leading jet with $|\eta| < 0.5$ as obtained from a UA1 jet finder with $R \simeq 0.4$. The spectra of triggered events and all events are shown in Fig. 9. Due to limited statistics in the minimum bias sample (only down-scaled trigger) also events selected by a tower trigger from the EMCAL are shown. However, in the current installation only half of the EMCAL is covered by TRD acceptance. The ratio of the triggered and untriggered sample shown in Fig. 9 must not be interpreted as a trigger efficiency since there is only a partial geometrical overlap of EMCAL and TRD at the current installation status.

7. Conclusions and Outlook

Based on first experience in pp data taking we have shown that the ALICE TRD is well suited to contribute physics triggers to the experiment at the level-1 stage. The main challenges lie in the very tight timing constraints, which require strict cuts already on the tracklet level. Furthermore, all calibration has to be applied on-line in the front-end electronics. This includes constant geometric corrections but also quantities varying with ambient conditions, such as the drift velocity which needs to be stabilized by an active feedback loop.

Further super-modules will be installed during the winter shutdown and increase the acceptance. Making use of the electron identification for the trigger contribution looks promising for future use.

References

- [1] ALICE TRD Technical Design Report, Tech. Rep. CERN/LHCC 2001-021, CERN (2001).
- [2] C. Blume, Commissioning and performance of the ALICE TRD, in: these proceedings.
- [3] Y. C. Pachmayer, Physics with the ALICE Transition Radiation Detector, in: these proceedings.

- [4] K. Aamodt, et al., The ALICE experiment at the CERN LHC, JINST 3 (2008) S08002. doi:10.1088/1748-0221/3/08/S08002.
- [5] X. Lu, Energy Loss Signals and Application in Particle Physics, in: these proceedings.
- [6] J. Stiller, Gain calibration of the ALICE TRD using a Krypton source, in: these proceedings.
- [7] V. Angelov, Design and Performance of the ALICE TRD front-end electronics, Nucl.Instrum.Meth. A563 (2006) 317–320. doi:10.1016/j.nima.2006.02.169.
- [8] S. Kirsch, F. Rettig, D. Hutter, J. de Cuveland, V. Angelov, V. Lindenstruth, An FPGA-based high-speed, low-latency processing system for high-energy physics, in: Field Programmable Logic and Applications, 2010, pp. 562 – 567. doi:10.1109/FPL.2010.110.
- [9] B. Heß, Online electron identification for triggering with the ALICE transition radiation detector, Diploma thesis, University of Heidelberg (2011).
- [10] AliRoot.
URL <http://alisoft.cern.ch/AliRoot/>
- [11] J. Klein, Commissioning of and Preparations for Physics with the Transition Radiation Detector in A Large Ion Collider Experiment at CERN, Diploma thesis, University of Heidelberg (2008).
- [12] O. Busch, DCS of the ALICE TRD, in: these proceedings.